PARTICLE DRAG FORCE IN A PERIODIC CHANNEL: WALL EFFECTS

M. Makhoul [1], P. Beltrame [1], M. Joelson [1]

[1] **Dept. Physique, UMR EmmaH 1114, Université d'Avignon et des pays de Vaucluse/INRA, F-84000 Avignon, France**

Abstract

This paper presents a computation of the drag force of a particle suspended in a periodic micropore channel, aimed at delineating the effects of the pore walls on the Stokes force. We treat the case of a spherical particle suspended in a newtonian fluid-filled tube whose diameter varies periodically, translating along the axis of the tube. The numerical computations, based on the integral equation formulation and coupling the traction and the velocity fields, are performed with a boundary-element method. An adaptive method is introduced to deal with the weak and strong singular integrals appearing in the mathematical formulation. These results allow to obtain an ordinary differential equation of the particle motion for arbitrary particle size.

Keywords: Microfluidic; Suspended particle; Stokes force; boundary integral equation; singular integrals.

1 Introduction

The Stokes force is known to be of main importance on the dynamics of particles suspended in a viscous fluid flow at low Reynolds number. Such situation is deserved in a wide range of applications concerning biology, environment and technology domains. The present work was motivated by a micro-pumping system [12] through periodic micropores channel. Recently, Beltrame and al. [13] show the role of the force drag in the existence of the particle transport. The model in the latter paper applies only in the case of fairly small particles. Our study aim at determining the validity of the latter model depending on the particle size and at presenting a generalization for arbitrary particle sizes.

In the past, various approximative modeling Stokes force on solid particles suspended in fluid flow was carried out with different analytical and numerical approaches. Using the method of perturbations, Brenner has calculated the Stokes resistance of a rigid particle with arbitrary geometric form suspended in a quasi-static flow, supposed at rest at infinity [1], in a shear flow [2], and in an arbitrary initial field flow [3]. The authors of [4] studied numerically by the Lattice-Boltzmann method the boundaries effect on the Stokes force of a sphere, undergoing a uniform translation motion outside the axis of revolution of the cylinder. Their numerical results agree with the experimental results obtained by Ambari [5], who proved that the force is minimal when the particle is on the axis of the cylinder and it increases quickly when the sphere approaches its boundaries. Nevertheless, Happel and Byrne have discussed in [6], the force, the torque and the pressure rise generated by the presence or the motion of a spherical particle or a periodic suspension of spherical particles in a cylindrical duct.

The present study deals with a more general configuration to compute the Stokes force on a spherical particle settling in an arbitrary channel form, filled with a viscous fluid flow at a very low Reynolds number, as long as the size of the particle is comparable to the size of the duct.

We solve this problem using the boundary integral method. The boundary integral method is particularly suited to solve Stokes flows with complex geometries. It is based on the viscous hydrodynamic potential theory introduced by Ladyzhenskaya starting from the Greens theorem results. Over the last three decades, the method was widely developed and matured. For instance, Kohr in [7] gave a boundary integral formulation to calculate the perturbation of an infinite incident flow in the presence of a solid sphere and a viscous drop, Jeffrey *et al.* [8], applied such formulation to compute the disturbance velocity field of a Poiseuille flow due to the presence of a sphere.

This paper is organized as follows: in the next two sections, we describe the boundary integral formulation of the problem and its numerical treatments. In the last section, we present our results and discussions.

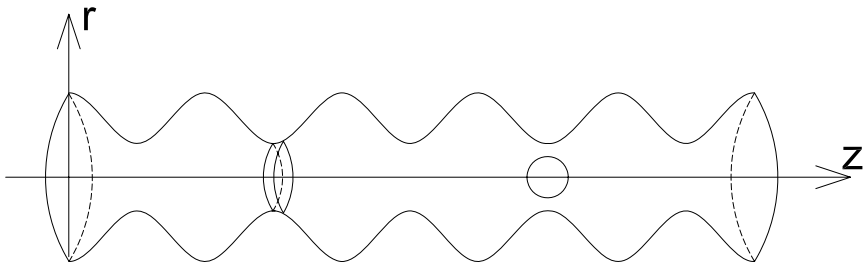

Figure 1: Sketch of the problem: a particle moves in the periodic micropore channel along the axis. The pore profile is given by the equation (1).

2 Boundary integral formulation and numerical resolution

We consider an incompressible viscous flow through a confining axisymmetric tube past a solid spherical particle. One tube is a subject of a number of interconnected identical pores with periodic variation in diameter as shown in figure 1. We are interested in such pores because they represent some kinds of realistic porous media [12].

We consider a channel with sinusoidal variations in radius, such as

$$r(z) = \frac{r_{min}}{2}\left[\sigma + 1 + (\sigma - 1)\cos(2\pi z/L)\right] \tag{1}$$

where L is the pore length, σ the ratio r_{max}/r_{min} called curvature of the pore. Note that $\sigma \geq 1$ and $\sigma = 1$ corresponds to an uniform cylindrical tube.

In this study, we deal with an incompressible quasi-static flow induced by a pressure gradient, periodically pumped back and forth. Indeed, considering the following characteristic values: the pore length L which is about 10μm, the mean velocity $U_m = L/T$ (T is the pumping period) ranging from 10^{-4} s to 10^{-2}, then the Reynolds number of a viscous fluid as water is small. Therefore, it is a creeping flow described by the Stokes equation and the continuity equation. Moreover, because of the fluid is viscous, we consider no-slip boundary condition. In the following, we work with dimensionless variables. The lengths are scaled by the pore length L, the time by the pumping period T and the pressure by the pressure difference $[p]$ imposed by the pumping.

Because of the fluid motion is linear, in order to compute the drag force, we compute first the velocity and pressure fields ($\vec{u}^0$,p^0) without particle and secondly the perturbation ($\vec{u}^d, p^d$) due to a single particle. As in [12], we consider a large number of pores, so that the incident velocity flow $\vec{u}^0$ can be assumed periodic. Then, if the pressure $[p]$ is given between the inlet and the outlet of the pore, there is an unique solution of the following problem:

$$-\vec{\nabla}p^0 + \Delta\vec{u^0} = 0 \tag{2}$$

$$\vec{\nabla}.\vec{u^0} = 0 \tag{3}$$

The boundary conditions are given by the non-slip condition on the lateral surface S^L of the channel, and the periodicity between the two ends,

$$\begin{aligned} \vec{u}^0 &= 0 \text{ on } S^L \\ \vec{u}^0(r,0) &= \vec{u}^0(r,1) \end{aligned} \tag{4}$$

The perturbed flow $(\vec{u}^d, p^d)$ due to the particle is governed by the equations (2) and (3) with the boundary conditions:

$$\begin{aligned} \vec{u}^d &= 0 \text{ on } S^L, \forall z \in [0,L] \\ \vec{u}^d(r,0) &= u^d(r,L) = 0, \forall r \\ \vec{u}^d &= u_p - u^0 \text{ on } S_p \end{aligned} \tag{5}$$

Because of the symmetry about the longitudinal axis of the channel, the cylindrical coordinates are chosen for the numerical description.

Owing to the fact of linearity we have in problem (2-3), the drag force, $\vec{F}$, acting on the particle may be decomposed into two parts,

$$\vec{F} = \vec{F_1} + \vec{F_2} \tag{6}$$

where $\vec{F_1}$ is the contribution of the initial and non disturbed flow, while $\vec{F_2}$ is due to the effect of the perturbed flow. The first term is written as following:

$$\vec{F_1} = \int_{S_p} \bar{\bar{\sigma}}.\vec{n}dS \tag{7}$$

where $\bar{\bar{\sigma}}$ denotes the stress tensor exerting on the surface of the particle:

$$\bar{\bar{\sigma}} = -p\bar{\bar{I}} + (\vec{\nabla}u + \vec{\nabla}u^T) \tag{8}$$

Using the Green formula and since the incident fluid is at equilibrium, one can show that the force $\vec{F_1}$ vanishes. In contrast, the second component $\vec{F_2}$ does not vanish. The latter force can be also written as sum of two contributions again because of linearity argument. The first one emphasizes the influence of the particle motion in the fluid, and the second one reveals the effect of the incident flow. In other words, the perturbed problem is solved as the sum of two problems with different boundary conditions on the particle surface. Firstly we take $u^d = u_p$ (moving particle in a fluid at rest), and secondly u^d = -u^0 (steady particle in a moving fluid). This decomposition allows us to write $\vec{F_2}$ as following:

$$\vec{F_2} = -\gamma(z)\left[u_p - U_{eq}(z)\right]\vec{e}_z \tag{9}$$

where z designates the position of the particle center, and the $\gamma(z)$ represents the coefficient of the drag force exerted on the particle. The velocity $U_{eq}(z)$ corresponds to the fluid velocity $\vec{u}^0$ in the limiting case of a point particle. Thus, this formulation generalizes the classical expression of the Stokes force which is justified for a particle radius negligible compared to the channel radius, i.e. the effect of the wall is not taken into account.

We are now in a position to find the solution $(\vec{u}^0, p^0)$ and $(\vec{u}^d, p^d)$ of the equations (2-3) with the boundary conditions (4) or (5). In the following, we omit the upper-script. The velocity field in the fluid is related to the velocity and tractions fields at the boundary domain by the integral equation:

$$u_k(\vec{x}) = \int_{\partial\Omega} t_i(y){U_i}^k(\vec{x},\vec{y}) - u_i(\vec{y}){T_i}^k(\vec{x},\vec{y}) \text{ for } k = r, z \text{ and } i = r, z \tag{10}$$

Where $\vec{t}$ and $\vec{u}$ represent the traction and velocity vectors respectively. T_i^k and U_i^k designate respectively the stress and velocity tensor associated to the elementary solution called Stokeslet. Physically, ${U_i}^k(\vec{x},\vec{y})$ $[{T_i}^k(\vec{x},\vec{y})]$ is the ith velocity [traction respectively] component at the point $\vec{y}$ due to a Dirac punctual force located at the point $\vec{x}$ pointing in the kth direction. General informations on boundary integral formulation for Stokes flow and its associated elementary solution can be found in [9, 10]. We note that the terms of U_i^k and T_i^k are singular as $|\vec{y} - \vec{x}|^{-1}$ and $|\vec{y} - \vec{x}|^{-2}$ respectively. The equation (10) can be properly used for $\vec{x}$ in the domain and not on the boundaries. The authors in [9, 10] give a regularized equation of (10), which contains just weak singular integrals and can be therefore valid for all $\vec{x}$ located on the boundaries.

The three main steps of the numerical implementation of the boundary integral equation are: the representation of the geometry with boundary elements, the discretization of the unknown traction and velocity fields, and the calculation of the integrals.

The starting point is to introduce a partition of the boundary $\partial\Omega$ into N_E boundary elements, $\partial\Omega = \cup_{e=1}^{e=Ne} E_e$, using $N_e + 1$ points and write the boundary integral equation (10) as a sum of elementary integrals. The fact that we are in 3D axisymmetric, our boundary elements are curved ones. The second point is the representation of the unknown vectors on the boundary, it gets the formalism of finite elements and leads to calculate the unknowns at the so called interpolation points. For convenience, we choose the points of geometric discretization for interpolation. For each point, N_k of these points, we associate an interpolation function $M_k(y)$, then we write an approximation of order 1 of the unknowns as:

$$u_i(y) = M_k(y)u_i(y^k) + M_{k+1}(y)u_i(y^{k+1}) \text{ if } y \in [y^k, y^{k+1}] \tag{11}$$

where $u_i(y^k)$, for k=1,,N_e+1, are the N_e+1 nodal values that we are going to compute.
Finally, the collocation method is employed in order to construct and solve numerically the discretized problem. It consists in forcing the equation (10) to be verified in certain points of collocation, $\vec{x}^c$, resulting a linear system of form $AX = B$. It is necessary to have at least equations as much as unknowns, so the simplest case is to choose the interpolation points as points of collocation from which a square linear system will be derived. This method involves regular elementary integrals when $\vec{x}^c$ is not in $[y^k, y^{k+1}]$, and singular ones when $\vec{x}^c$ belongs to $[y^k, y^{k+1}]$. For regular integrals, the gauss quadrature is applied, otherwise, a specific method is introduced in next section 3.

3 Singular integrals treatment

An elementary integral is singular when $\vec{x}$ belongs to the boundary element of integration. In the past, a plethora of works have be done to treat the singular integrals. We choose the approach developed by Guiggiani *et al.*[11] which has the advantage to be quite generic. The use of the regularized equation of (10), given in [9, 10] allows us to deal only with weak singular integrals.
The technique to calculate the weak singular integrals is based on the introduction of a polar system coordinates, (ρ,α), centered at the singular point, or the collocation point. Note that the cylindrical coordinates (r, θ, z) do not match the polar coordinates tangent to the pore surface. Using the Taylor expansion, we can show that the square of the distance d between two the collocation point and the integration point can be written as following:

$$d^2(z,\theta) = \rho^2(z,\theta) + o(\rho^2(z,\theta)) \tag{12}$$

where $\rho(z,\theta)$ is:

$$\rho(z,\theta) = \sqrt{(1+H(z_c)^2)(z-z_c))^2 + (r(z_c)\theta)^2} \tag{13}$$

The function $r(z)$ appearing in (13) designates the pore radius, $H(z)$ its derivate. (z,θ) are the cylindrical coordinates of the integration point, and (z_c,θ=0) are those of the collocation point. The equation (13) helps us to perform the following change of variables :

$$(1+H(z_c)^2)(z-z_c) = \rho\cos\alpha \tag{14}$$

$$(r(z_c)\theta) = \rho\sin\alpha \tag{15}$$

The main idea of this method is to isolate the singular kernel of U_i^k tensor and expresses it with the new variables ρ and α, it is a kind of Laurent series:

$$U_i{}^k(z,\theta) = \frac{f(\alpha)}{\rho(z,\theta)} + b_1(z,\theta) \tag{16}$$

where $b_1(z,\theta)$ is a bounded function. Then, the second term of the right hand side of (16) can be computed using a classical gauss quadrature formula. For the first term, the weak singularity is removed using a polar change variables involving ρ and α.

4 Results and discussions

In order to study the effect of the wall on the force and to have analogy with the Stoke's force, the force is written as sum of two contributions, as we already mentioned in (9), i.e. the drag $\gamma(z)$ and the equivalent velocity field $U_{eq}(z)$. We, first, compare the results with analytical expansions in the literrature for a spherical particle in a cylindrical tube, see e.g. [6]. According to their results, if ϵ, the ratio of the particle radius over the channel radius, is small then we have:

$$\gamma/\gamma_0 = \frac{1}{1-2.105\epsilon+2.087\epsilon^3}, \tag{17}$$

$$U_{eq}/U^0_{axis} = \frac{1-2/3\epsilon^2}{1-2.105\epsilon+2.087\epsilon^3}, \tag{18}$$

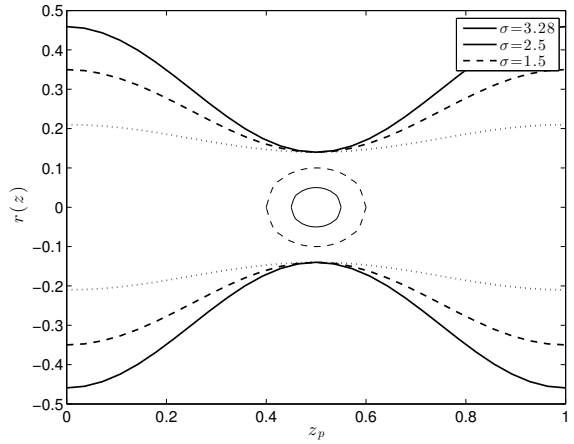

Figure 2: Pore profiles for $r_{min} = 0.14$ and three different mean curvatures $\sigma = 1.5, 2.5$ and 3.28. The circle correspond to the particle with the radius $R_p = 0.05$ and $R_p = 0.1$.

where γ_0 is the Stokes drag in an infinite domain and U^0_{axis} is the incident Stokes flow along the cylinder axis. As expected, the results agree with the expression for small ratios ϵ. In particular, the Stokes drag increases when the pore walls are closer. These series expansions remain a good approximation for quite large ϵ. But, for $\epsilon > 0.2$ the computed drag differs more than 10% from the one given by the previous expression. Note, that the drag is an increasing function for all ratio ϵ contrary to the approximation (17).

Now, we consider a channel with sinusoidal radius variations given by Eq. (1). The studied profiles are displayed in figure 2. The minimal radius r_{min} is fixed while three different mean curvatures of the pore are considered. The drag γ and the equivalent velocity profiles U_{eq} depend on the z position of the particle. The figures 3 and 4 display these variations for two particle radii: $R_p = 0.05$ and $R_p = 0.1$. The maxima of γ and U_{eq} coincide to the bottle-neck of the channel while the minima of these quantities correspond to the largest radius of the pore. These results are in the same vein as for the cylindrical channel: a narrower channel leads to a larger drag. Moreover the drag coefficient increases when the curvature decreases and it is maximal for $\sigma = 1$ which corresponds to the case of a cylinder. For instance, the drag on a particle of radius 0.1 in a cylinder of radius equal to r_{min} is equal to 25.17 which is greater than the maximal values presented in figure 4.

In order to discuss the simple model proposed in [13] for the particle transport in a periodic channel, let us introduce a measure of the relative variation of a quantity Q which is called contrast:

$$c_Q = \frac{Q_{max} - Q_{min}}{Q_{max} + Q_{min}}. \tag{19}$$

The contrast ranges from zero which corresponds to the case where Q is constant, to one which obtained when $Q_{min} = 0$. In [13], it is shown that the particle transport may arise for a velocity contrast $c_{U_{eq}}$ large enough about 0.6 while the drag coefficient γ is assumed constant. According to figures 3 and 4 the contrasts c_γ and $c_{U_{eq}}$ increases with the curvature σ. If we compare for a same pore geometry the equivalent velocity for two different particles radii, then the contrast $c_{U_{eq}}$ decreases for larger particles. This result is expected since this velocity field corresponds to a kind of a mean effect of the fluid velocity field over the particle domain. Concerning the particle drag, its value increases dramatically with the particle radius: there is a ratio about 3 or 4 between two drags of particle of different sizes with the same pore geometry. We found that for a small particle $R_p = 0.05$, the velocity contrast varies from 0.3 to 0.66 approximatively when the pore curvature varies from 1.5 to 3.28. The drag contrast is not negligible but small about 0.1 and remains inferior to 0.18. Then, the assumption of [13] could be realized for σ about 3. If the particle size is larger ($Rp = 0.1$), the velocity contrast is slightly lower: its maximal value is still 0.6 for $\sigma = 3.28$. However, the drag contrast is about 0.3 and then its spatial variations are no more negligible. Then, according to Eq. (9) and assuming that a slow sinusoidal pumping is applied, the motion

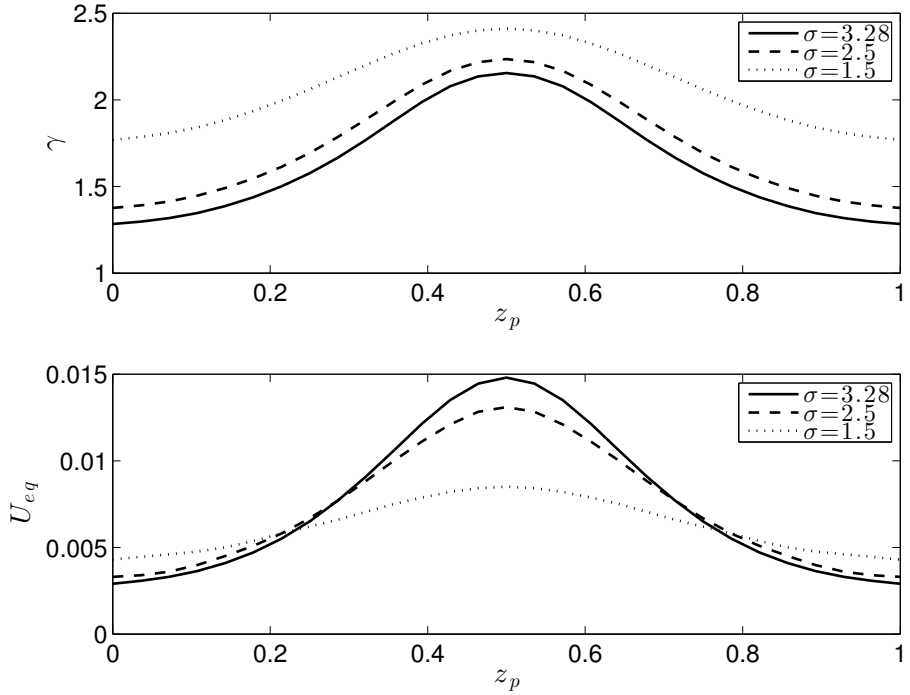

Figure 3: Spatial variation of the drag $\gamma(z)$ and the equivalent velocity field $U_{eq}(z)$ of a particle of radius $R_p = 0.05$ along the axis. The three different pore profiles of figure 2 are considered.

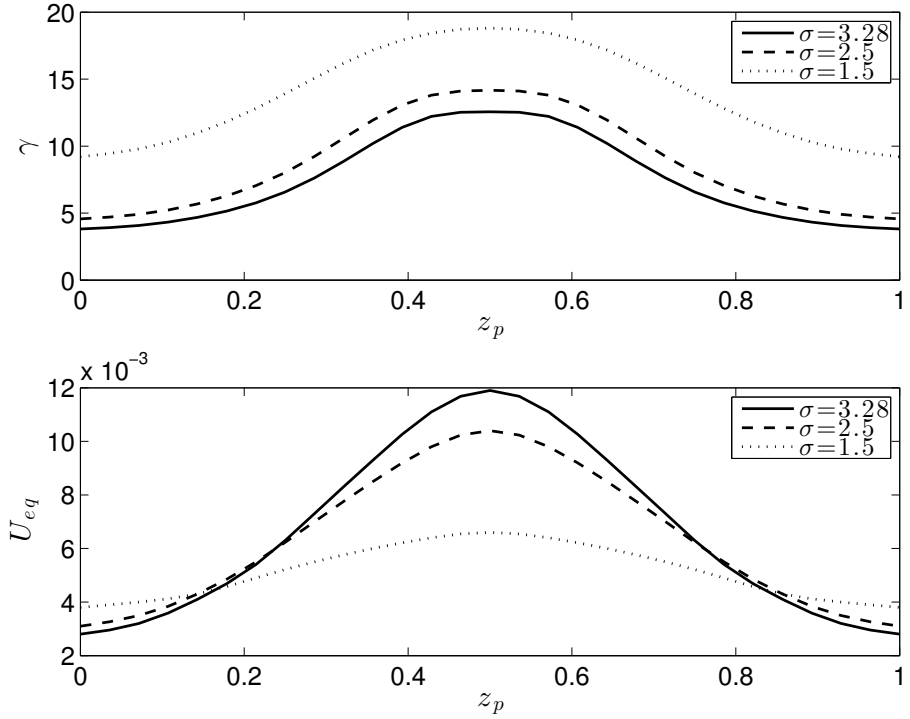

Figure 4: Spatial variation of the drag $\gamma(z)$ and the equivalent velocity field $U_{eq}(z)$ of a particle of radius $R_p = 0.1$ along the axis. The three different pore profiles of figure 2 are considered.

of a particle of mass m is governed by the nonlinear differential equation:

$$m\ddot{z} = -\gamma(z)\left[\dot{z} - U_{eq}(z)\sin(2\pi t)\right]. \tag{20}$$

This equation differs from the model in [13] only by the spatial variation of γ. Therefore, the same bifurcation analysis to study the particle dynamics and its transport may be applied. Moreover, the equation (20) may be applied for any particle size contrary to the model in [13].

5 Concluding remarks

We have developed a numerical code using boundary elements for the estimation of the drag force on a particle of arbitrary size in a confined periodic channel. Our numerical results point out that even in the case of a cylindrical duct, analytical approximations cannot estimate properly the drag force for particle radius larger than one-fifth of the duct radius. Thus, numerical computation of the drag force is needed. We show that the drag force can be characterized by two quantities: the friction coefficient $\gamma(z)$ and the equivalent velocity field $U_{eq}(z)$. Both quantities depend on the z position of the particle. We study them for different pore shapes defined by the curvature. We focus especially on their spatial variations called contrast in order to compare with the model of particle transport used in [13]. We show that this latter model of this latter applies only for small enough particles. Nevertheless, the knowledge of γ and U_{eq} allows to get a non-linear equation of second order to describe the particle motion as in [13]. Thereby, similar system dynamical tools may be employed in order to find and understand the transport mechanisms of a particle in a periodic micropore channel. One should note, that the direct numerical simulation of such a problem was performed by [14]. However, this method increases dramatically the CPU cost comparing to our present approach. It is crucial especially when an intermittent transport (drift ratchet) occurs because a longtime integration is required to display the slow particle drift.
Note finally that even if the present work focused on the case of spherical particle, our method could be applied to an arbitrary axisymmetric shape of the particle. That, will be studied in a further work.

References

[1] Brenner, H.: Effect of finite boundaries on the Stokes resistance of an arbitrary particle Part 2. Asymmetrical orientations. *Journal of Fluid Mechanics*, vol. 18, no. 01: (1964) pp. 144–158.

[2] Brenner, H.: The Stokes resistance of an arbitrary particle-III Shear fields. *Chemical Engineering Science*, vol. 19, no. 09: (1964) pp. 631–651.

[3] Brenner, H.: The Stokes resistance of an arbitrary particle-IV, Arbitrary fields of flow. *Chemical Engineering Science*, vol. 19, no. 10: (1964) pp. 703–727.

[4] Godin,Th., Bouzidi, M., Lallemand, P. & Ambari, A.: Numerical calculation of wall effect and backflow on the Stokes force. *Comptes Rendus Mécanique*, vol. 330, no. 12: (2002) pp. 837–842.

[5] Ambari, A., Gauthier-Manuel, B. & Guyon, E.: Wall effects on a sphere translating at constant velocity. *Journal of Fluid Mechanics*, vol. 149, no. 12: (1984) pp. 235–253.

[6] Happel, J. & Byrne, B.J.: Motion of a sphere and fluid in a cylindrical tube. *Industrial & Engineering Chemistry*, vol. 46, no. 6: (1954) pp. 1181–1186.

[7] Kohr, M.: Boundary integral method for a Stokes flow past a solid sphere and a viscous drop. *Computer Methods in Applied Mechanics and Engineering*, vol. 190, no. 42: (2001) pp. 5529–5542.

[8] Schonberg, J. A., Drew, D. A. & Belfort, G.: A neutrally buoyant sphere in creeping flow between parallel plates: farfield velocity profiles. *Chemical Engineering Science*, vol. 45, no. 1: (1990) pp. 225–235.

[9] Bonnet M.: Boundary integral equation methods for solids and fluids. *Wiley-Blackwell* (1999).

[10] Pozridikis, C.: Boundary integral and singularity methods for linearized viscous flow. *Cambridge University Press* (1992).

[11] Guiggiani, M., Krishnasamy, G., Rudolphi, T. J. & Rizzo F. J.: A general algorithm for the numerical solution of hyper singular boundary integral equations. *Journal of Applied Mechanics* vol. 59, no. 3: (1992) pp. 604–614.

[12] Kettner, Ch., Reimann, P., Hänggi, P. & Müller, F.: Drift Ratchet. *Phys. Rev. E* vol. 61, no. 1: (2000) pp. 312–323.

[13] Beltrame, Ph., Talkner, P. & Hänggi, P.: Deterministic transport of particles in a micro-pump. *Preprint arXiv:1205.4339*

[14] Brenk, M., Bungartz, H.-J., Mehl, M., Muntean, I. L., Neckel, T. & Weinzierl, T.: Numerical Simulation of Particle Transport in a Drift Ratchets *SIAM J. Sci. Comput.*, vol. 30: (2008) pp. 2777–2798